The Astrophysical Journal, 811:1 (5pp), 2015 September 20 doi:10.1088/0004-637X/811/1/1

A STATISTICAL SEARCH FOR A POPULATION OF EXO-TROJANS IN THE *KEPLER* DATA SET

Michael Hippke[1] and Daniel Angerhausen[2,3]
[1] Luiter Straße 21b, D-47506 Neukirchen-Vluyn, Germany; hippke@ifda.eu
[2] NASA Goddard Space Flight Center, Greenbelt, MD 20771, USA; daniel.angerhausen@nasa.gov
Received 2015 June 8; accepted 2015 August 4; published 2015 September 11

ABSTRACT

Trojans are small bodies in planetary Lagrangian points. In our solar system, Jupiter has the largest number of such companions. Their existence is assumed for exoplanetary systems as well, but none have been found so far. We present an analysis by super-stacking $\sim 4 \times 10^3$ *Kepler* planets with a total of $\sim 9 \times 10^4$ transits, searching for an average Trojan transit dip. Our results give an upper limit to the average Trojan transiting area (per planet) that corresponds to one body of radius <460 km with 2σ confidence. We find a significant Trojan-like signal in a subsample for planets with more (or larger) Trojans for periods >60 days. Our tentative results can and should be checked with improved data from future missions like *PLATO 2.0*, and can guide planetary formation theories.

Key words: minor planets, asteroids: general – planets and satellites: general

1. INTRODUCTION

In 1771, the mathematician Lagrange found a solution to the three-body-problem for a primary planet and an asteroid of small mass. When the bodies are in the same plane in circular orbits of the same period, the stable locations for the asteroid are 60° from the planet (Lagrange 1772). As no such asteroids were known at the time, the problem was considered to be only of mathematical interest. Today, we refer to these points as the (stable) Lagrangian points L4 and L5 (Figure 1, based on Cornish 1998).

More than a century later, Max Wolf (1996) of the University Observatory of Heidelberg discovered a new "planet" 55° east of Jupiter and immediately noted its strange orbit: "the small change in R.A. is remarkable."[4] More such bodies were found in the same year, and it was quickly realized that these bodies are trapped in Jupiter's Lagrangian points. To distinguish them from the main belt asteroids, which usually receive female names, it was decided to name them after Greek heroes of the Trojan war. Wolf's "planet" is today known as (588) Achilles and is in the L4 group.

Asteroids that are trapped in an L4 or L5 orbit around their point of equilibrium have a tadpole or horseshoe orbit (Marzari et al. 2002). Today, >6000 Jupiter Trojans are known[5], as well as a few Neptune, Mars, and Earth Trojans. The largest known Trojans have sizes >100 km in radius (Fernández et al. 2003), and it is believed that the total number of L4 Jupiter Trojans, with radii >1 km, is $\sim 6 \times 10^5$ (Yoshida & Nakamura 2005). If L5 contains an equal amount of debris, then the total transiting area equivalent of small Jupiter Trojans corresponds to one body of radius ~600 km. The 32 largest objects (Fernández et al. 2003) account for an additional radius equivalent of ~300 km.

The Lagrangian points are stable over Gyr timescales as long as the planet is <4% of the system mass (Murray & Holman 1999). Most of the system mass is usually concentrated in the host star, e.g., 4% of $M_\odot$ is $40 M_{\rm Jup}$, so that this limit is usually met. Consequently, we might assume that other planetary systems also possess Trojan bodies; this is also expected from formation mechanisms in protoplanetary accretion discs (Laughlin & Chambers 2002). As the properties of extrasolar systems are diverse, we can ask the question of how large these bodies can be, and how many there are. There is nothing that physically prevents them from occurring in larger numbers (and/or larger sizes) than in our own system. Hypothetical exo-Trojans have been shown to be stable for up to Jupiter mass in the most extreme cases (Érdi et al. 2007), assuming low eccentricity (Dvorak et al. 2004).

Searching for Trojans in time series photometry is difficult, as these bodies librate around their equilibrium points to a substantial degree. This produces large transit timing variations, so they are missed in standard planet-search algorithms. Also, the mean inclination of Jupiter Trojans is 10° (Yoshida & Nakamura 2005) to 14° (Jewitt et al. 2000). If this is typical for exo-Trojans, only part of the swarm would go into transit.

Data from the *Kepler* space telescope have been searched for individual Trojans, with a null result and sensitivity down to $\sim 1 R_\oplus$ (Janson 2013). Another search was carried out with data from the *MOST* satellite for the transiting hot Jupiter HD 209458b, also with a null result and an upper limit of ~1 lunar mass of asteroids (Moldovan et al. 2010).

Although interesting, we do not repeat these searches for individual Trojans here, but ask the question of the *average* Trojan effect in all *Kepler* data. Millions of small Trojans might show up, on average, when stacking $\sim 4 \times 10^3$ planets with a total of $\sim 9 \times 10^4$ transits, as is the case for exo-moons (Hippke 2015).

2. METHOD

We employed the largest database available: high precision time series photometry from the *Kepler* spacecraft, covering 4 years of observations (Caldwell et al. 2010).

2.1. Data Selection

Based on a list of all validated transiting *Kepler* planets (821) and unvalidated planet candidates (3359; Wright et al. 2011)[6],

[3] NASA Postdoctoral Program Fellow.
[4] In the original German: "Bemerkenswerst ist (...) die kleine R.A.-Bewegung von TG."
[5] IAU Minor Planet Center, http://www.minorplanetcenter.net/iau/lists/JupiterTrojans.html, list retrieved on 2015 April 26.
[6] http://www.exoplanets.org, list retrieved on 2014 November 18.

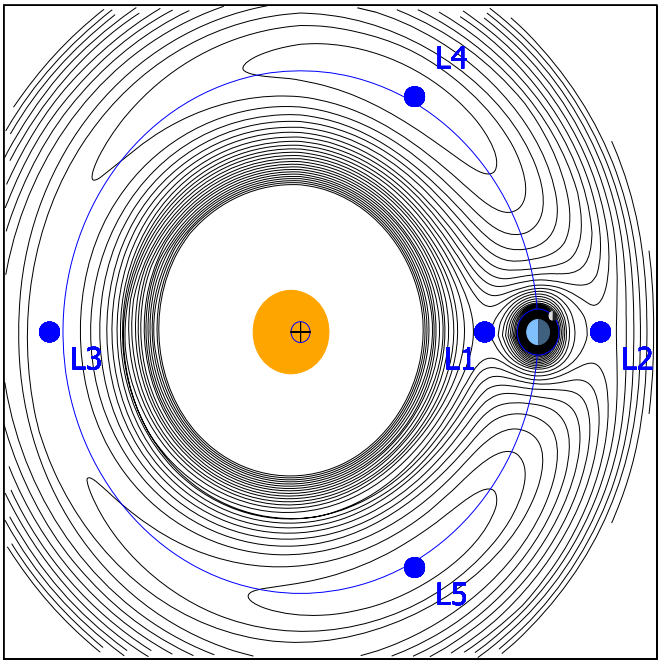

Figure 1. Lagrangian points L4 and L5 are 60° from the planet.

we downloaded their *Kepler* long-cadence (30 minutes) data sets. We used the same data set as published by the Transiting Planet Search pipeline, which relies on a systematic error-corrected flux time series from a "wavelet-based, adaptive matched filter that characterizes the power spectral density (PSD) of the background process yielding the observed light curve and uses this time-variable PSD estimate to realize a pre-whitening filter and whiten the light curve" (Borucki et al. 2011). This data set was used for most planet validations (e.g., Lissauer et al. 2012; Rowe et al. 2014). We have downloaded these data from the NASA Exoplanet Archive[7] and applied no further corrections or detrending. It must be assumed that there are unidentified transits and stellar trends in these data, but we can also assume that these are distributed randomly over phase time, so no systematic effects should affect the precise locations of the L4 and L5 phase times.

2.2. Data Processing

Each planet has its own light curve in this data set, which comes with companion transits removed (in multiple systems). We phase-folded every light curve with its published period. Afterward, we re-normalized the data for each curve, while masking the times around planetary primary and secondary transit. Then we re-binned each phase-folded light curve in 1000 bins. Depending on the period, this is equivalent to a time of 1 minute (for the shortest period) to 18 hr (for a 750-day period). For the median period of 13 days, the bin length is 20 minutes. As the average transit duration is a few hours, smearing only occurs for the few very long period planets.

2.3. The Super-stack

From the sample of 3739 useful phase-folded light curves in 1000 bins, we created a super-stack by co-adding these and taking the median of each bin. This method was also used by Sheets & Deming (2014) for the detection of average secondary eclipses, and by Hippke (2015) for the search for an average exo-moon effect. In contrast to these studies, we did not stretch to the expected transit duration because Trojans are expected to be in orbits around the Lagrange-points, and not stationary in phase time.

[7] http://exoplanetarchive.ipac.caltech.edu/docs/API_tce_columns.html, retrieved on 2015 April 21.

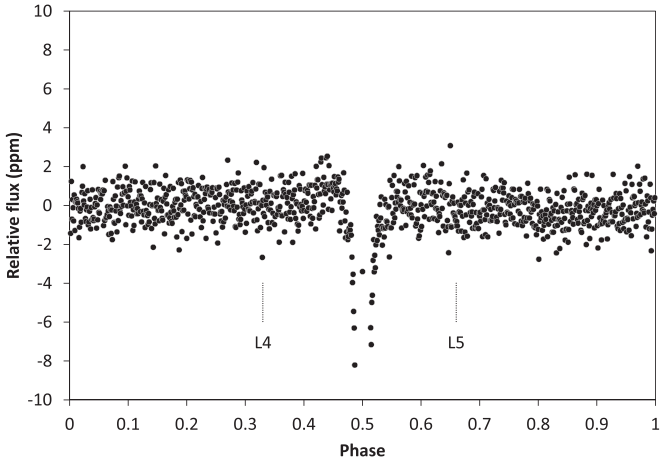

Figure 2. Initial super-stack shows no significant dips at the Lagrangian points.

The resulting data were strongly dominated by outliers. This is caused by many factors contributing to different noise levels: the brightness of the host star, stellar variability, instrumental differences, and others. We decided on two filters to remove outliers, namely the stellar brightness (we kept stars brighter than 15 mag in J as measured by 2MASS), and the scatter per star (we kept the better half).

It is interesting to mention a (slight) selection effect from this filter choice: When rejecting dimmer and/or noisier stars, the average stellar radius changes. Smaller stars (e.g., M-dwarfs) exhibit more stellar noise (Basri et al. 2013) and are usually less luminous. Consequently, our sample is shifted toward larger stellar radii. While the total *Kepler*-planet sample has an average stellar radius of $1.14 R_{\odot}$, our post-filter sample has an average of $1.17 R_{\odot}$.

3. RESULTS

The initial post-filtered super-stack does not show any significant Trojan dips, as shown in Figure 2. When taking the average flux in a bin of 0.03 width in phase space, we obtain $+0.06 \pm 0.23$ ppm for L4 and -0.10 ± 0.23 ppm for L5. For the average stellar radius of $1.17 R_{\odot}$, we can set an upper limit for the average Trojan area (per planet) of 460 km with 2σ confidence. This applies to the full (filtered) *Kepler* sample.

3.1. Cross-check for Secondary Eclipses

As a useful cross-check for our data preparation method, we have searched for the average secondary eclipse. For simplicity, we have assumed only reflected light with an average albedo of 0.22 (Sheets & Deming 2014) and neglected differences in temperatures. As can be seen in Figure 2, there is only a hint of a secondary features at phase $1.0 = 0.0$, which is measured to be -0.31 ± 0.21 ppm at a bin width of 0.01. Following our simplified assumptions, we can calculate the expected dip for this sample as $(R_P/a)^2$ per planet, giving an average of -0.88 ppm for the sample. We explain the

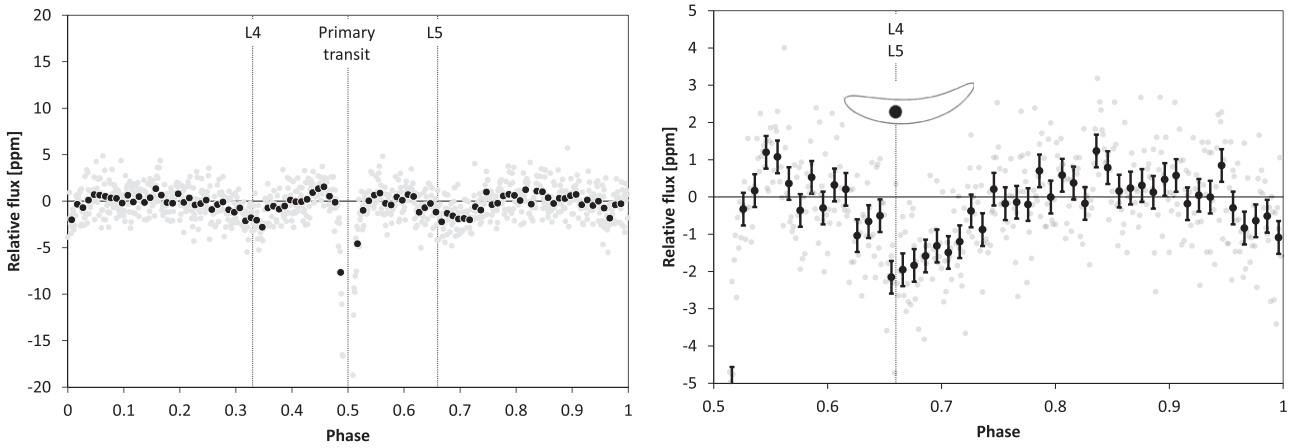

Figure 3. Sub-sample super-stack in normal (left) and double symmetric (right) phase fold, with expected orbit size shown for reference. Note the different vertical axes. The gray dots are 1000 bins over phase space, and the black dots with error bars (right) are 100 bins for better visibility.

difference as caused by smearing from shifts in transit timing (from non-zero eccentricity) and different transit durations of each planet, which we did not compensate for.

We have also checked a different sample that is expected to yield a higher secondary dip: all planets with radii $>2R_{\oplus}$ on orbits <0.3 AU. This sub-sample is expected to yield an average secondary eclipse of -1.7 ppm; our data analysis gives -0.73 ± 0.34 in the same bin width. Again, we have to expect centering variations that reduce (broaden) the observed depth. However, it is reassuring to see a dip at $>2\sigma$ significance. Finally, we have checked the few individual examples from Sheets & Deming (2014) where the secondary eclipse is detected for individual planets (e.g., Kepler-10b); these dips are also present in our data set. We conclude that there seems to be no obvious fault in our data set, and that secondary eclipses are hard to detect for most of the *Kepler* planets.

3.2. Sub-sample Analysis

The full sample might be heavily diluted by a large number of systems with no or relatively few Trojans. We test this hypothesis by assuming that the flux in L4 and L5 is uncorrelated for any cause other than Trojan bodies. We know from our own solar system that the number of bodies in L4 and L5 is approximately equal. Then we can examine a sub-sample of the super-stack: we take all of those planets that exhibit a negative flux at L4 (phase 0.33), and take their data of phase 0.5–1 for further analysis. The same is done for L5 in the reverse logic. This gives us 1251 samples of negative flux at phase 0.33, and their light curves for the "right part," i.e., flux phase 0.5–1. We also find 1266 samples with a dip at phase 0.66, and take their part of the light curves from phase 0–0.5. Afterwards, we stitch these halves together, and obtain 1940 light curves (some have dips in both halves). The result of this sub-sample is shown in Figure 3 and exhibits a clear dip at both L4 and L5, with a maximum depth of 2 ppm (970 km radius equivalent). It is reassuring to see that this dip is not uniform; as can be seen in the double-phase fold (right part of this figure), its shape is elongated away from planetary transit, as is expected for distributions from horseshoe and tadpole orbits.

An alternative interpretation of the dips in Figure 3 (left) would be numerical fluctuations caused by autocorrelation. Indeed, a Durbin–Watson test returns clear autocorrelation ($p = 0.01$) if the complete data set of 1000 bins is used. However, when we excise the phase times with signals (around 0, 0.33, 0.5, 0.66, and 1) and treat only the remaining data, then autocorrelation is insignificant even at the 10% level.

We have also cross-checked whether this dip is introduced by some symmetry artifact. When selecting any other phase-folded time, e.g., flux <0 at phase 0.2, no equivalent dip on the "other side" of the orbit, i.e., at phase 0.8, can be reproduced. Figure 4 shows this: if an artifact were present, we would expect a dip centered at each black mark, which is not present. Clearly, we cannot produce a similar dip at any phase time with this symmetry argument; it only works at phase times 0.33 (L4) and 0.66 (L5). We caution, however, that the signal-to-noise ratio (S/N) of the total signal is low, as will be explained in the following section. Splitting such a weak signal into different views can therefore only create weak indicators of its validity.

3.3. Significance of the Result

To measure the significance of these dips, we take the S/N for transits (Jenkins et al. 2002; Rowe et al. 2014), which compares the depth of the transit mode compared to the out-of-transit noise:

$$\mathrm{S/N} = \sqrt{N_T}\frac{T_{\mathrm{dep}}}{\sigma_{OT}}, \quad (1)$$

with N_T as the number of transit observations, T_{dep} as the transit depth, and σ_{OT} as the standard deviation of out-of-transit observations. For the Lagrangian signals, we find that the L4 and L5 dip at $\mathrm{S/N} \sim 6.7$ each, and a combined $\mathrm{S/N} = 9.3$. It has been argued by Fressin et al. (2013) that the detection of transits becomes unreliable for an $\mathrm{S/N} \lesssim 10$, so this signal can only qualify as a tentative detection.

3.4. Sub-sample Properties

We have compared the properties of the 1940 planets in our sub-sample to the total *Kepler* sample. We use a nonparametric density estimation with a local polynomial regression to include local confidence bands (e.g., Ruppert et al. 2003; Takezawa 2006).

We find a correlation of the Trojan-like dips to the period of the host star: At $p > 20$ days, the probability density moves toward more pronounced Trojan-like signal, but the effect becomes only formally significant for $60 < p < 350$ days (see

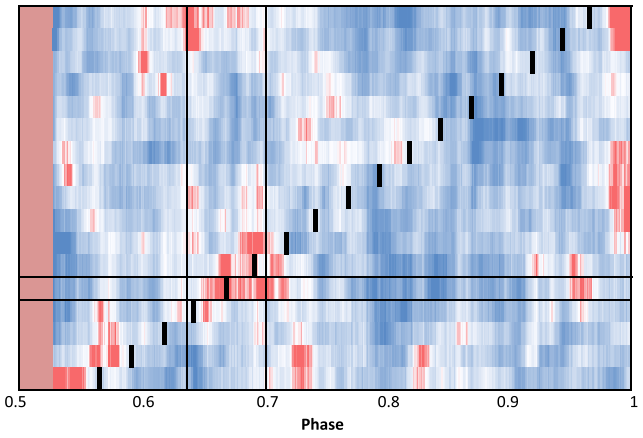

Figure 4. Cross-check of sub-sample selection artifacts. In each line, we select those data that have a dip on one side of phase space, and plot their flux only for the other half of phase space. For example, in the first row, all data are shown that have a dip at phase 0.034 (at boxcar width 0.03). If an artifact were present, we would expect a corresponding dip (red color) at phase $1 - 0.34 = 0.966$, which is not seen. Also, we would expect such an artifact to occur in every line, centered at the black marked, which is not the case. Instead, we mainly see red dips occur at phase ∼0.66, where the Trojan transits are expected. A few columns (0.025 in phase time) around primary transits are excised as these values are ∼1000× deeper in flux, making them incompatible with useful color scalings.

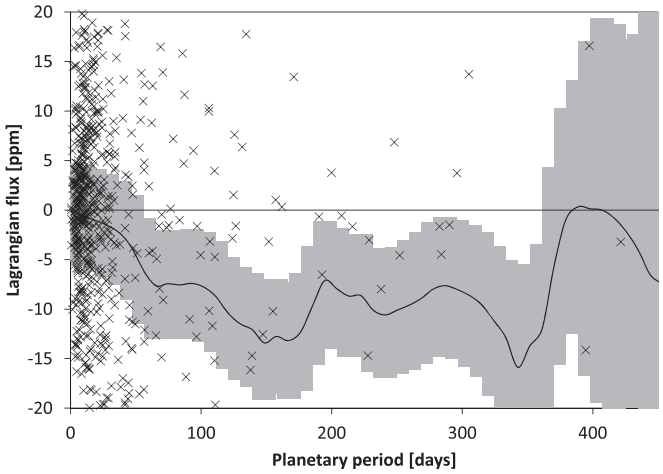

Figure 5. Density estimate for the Trojan-like signal vs. planetary period. The shaded area is the local 2σ confidence band. Short periods <50 days are consistent with zero Trojan signal, but a Trojan-like signal is detected for periods between 60 and 350 days. Uncertainty increases for longer periods due to a lack of data. See the text for a discussion.

Figure 5). This might either reflect a stability dependence of Trojan bodies to their semimajor axis, or a formation bias, or a mix of both. Due to radiation effects (such as the Yarkovsky effect (Bottke et al. 2006), which can cause small objects to undergo orbital changes), we can expect few (if any) close-in ($p < 10$ days) small asteroids. For long periods, $p > 350$ days, the sample size is too small for a significant result.

We have tried the same density estimates for several other measures, but all are formally insignificant. At first glance, for example, one might assume that the impact parameter of the planetary transit could positively affect Trojan detectability: for more central planetary transits, one might assume a sky-coplanar Trojan to also (more likely) transit centrally, making detection easier. However, this is likely overpowered by the inclination scatter of possible Trojan "swarms." If we take the inclination scatter of Jupiter's Trojans as a proxy, then the projected size of a Trojan cloud in exoplanetary systems would be several times larger than the projected size of their star. Given our data quality, it is not surprising to find no significant correlation with respect to the impact parameter.

The same argument can be made for a correlation with the stellar radius. One might hypothesize that the total Trojan mass correlates with the total mass of the circumstellar disk, which itself might be correlated with the mass of the star. More massive stars are known to host more massive planets (Johnson et al. 2010), so that Trojan bodies might also be more massive (i.e., larger at a given density). The scale for such a correlation, however, is expected to be of order $R_{\rm trojan} \sim M_{\rm trojan}^{1/3}$. The majority of *Kepler* planets and candidates are found for stars between $0.5R_*$ and $2R_*$, a range which, in combination with the limited data quality, does not allow for the detection of a significant correlation of Trojan occurrence to the stellar radius.

Finally, we also tried correlations to the planetary radius, multiplicity, metallicity of the host star, and eccentricity; all of which gave null results.

4. DISCUSSION

While the data quality from *Kepler* is the best we have, it is only barely sufficient for searching for Trojan bodies. Still, we believe that the methods outlined in this paper will be valuable in the future, when more and better data become available. The *PLATO 2.0* mission (Rauer et al. 2014) will deliver photometry for 500 bn stars in the years after 2024, and up to 3× better photometric precision. With such a data set, the analysis performed here should be repeated and should yield highly significant results for every breakdown. Also, a few single large Trojans might also be expected if the vast data set (Hippke & Angerhausen 2015) can be mined sufficiently.

We have explored the potential of *PLATO 2.0* using lower-limit estimates from Rauer et al. (2014) for its scientific return. Then, ∼10× more light curves will be available, when compared to *Kepler*, for a duration of 6 (instead of 3) years. For simplicity, we neglect the better instrumental noise properties. This gives $1/\sqrt{2 \times 10}$ of noise improvement per bin (compared to the current data), resulting in ∼0.3 ppm of noise in each of the 1000 bins. Consequently, from a super-stack without any selections, we can expect equal or better signal-to-noise properties than in the heavily selected and biased *Kepler* sample. More precisely, the full *PLATO 2.0* sample is expected to yield a signal-to-noise as shown in Figure 3, without any of our discerning selection choices.

Furthermore, we can expect to make clear detections of large individual Trojans with *PLATO 2.0*, if such bodies exist with transiting areas $>0.5R_\oplus$. To show this, we have created a series of injections. Our process is similar to the one described in Hippke & Angerhausen (2015). In short, we take real solar data from *VIRGO/DIARAD* (Fröhlich et al. 1997) and add instrumental noise from an end-to-end *PLATO 2.0* simulator (Zima et al. 2010; Marcos-Arenal et al. 2014). Into these data, we inject synthetic Trojan light curves, which are assumed to orbit in horseshoe orbits around L4/L5 with semimajor axes of ∼0.02 in phase time (Janson 2013). To explore the parameter space of recoverable signals, we varied the transiting Trojan area (radius), the stellar radius, and the planetary period. We show an exemplary riverplot in Figure 6 for a Sun-like star, orbited by a 10-day hot Jupiter and a $0.8R_\oplus$ Trojan in L4. Such

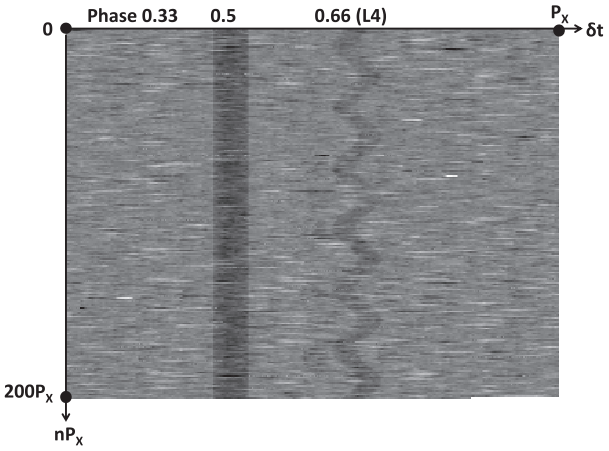

Figure 6. Riverplot of Trojan injection into 6 years of real solar data, assuming *PLATO 2.0* instrumental performance. A synthetic 10-day period hot Jupiter is visible at phase 0.5; the injected $0.8R_\oplus$ Trojan is clearly visible in its horseshoe orbit at L4.

a configuration is easily detected with visual examination, but might escape standard transit detection algorithms due to the large transit timing variations. We find that for Sun-like stars, transiting areas of $>0.65R_\oplus$ (Mars-size) are easily detected visually; the equivalent limit for a $0.5R_\odot$ M-Dwarf is $\sim 0.5R_\oplus$. Instead of a visual search, algorithms might be used, as explained by Janson (2013). However, it is unclear how efficient these can be; this would have to be determined with a series of injections and (blind) retrievals.

An interesting finding from our own injections is that potential Trojans at shorter period planets are much more easily identified due to their higher number of transits. Our example uses a 10-day planet; this is on the lower end of our hypothesized limit of planets having Trojans, as explained in Section 3.2. For longer period planets, e.g., a 100-day planet, the number of rows (transits) in Figure 6 would be 20 (instead of 200) for 6 years of data. This reduces the chances of detection, highlighting the benefits of long-term campaigns.

5. CONCLUSION

With the given data set, we only find a significant Trojan-like signal when applying the "left-right" method, selecting only L5 data for those candidates that seem to exhibit a L4 dip (and vice versa). While we tested this method to be robust against a symmetrical bias, it also implies that the main sample must be heavily diluted with a large number of systems with no (transiting) Trojans. If the method is valid, then the breakdowns of this sub-sample indicate that Trojans are more prominently found for longer (>60 days) periods. These cautious and preliminary findings might inspire theorists to advance planetary formation theory in that direction; these theories can then be validated with the upcoming data from the *PLATO 2.0* spacecraft.

REFERENCES

Basri, G., Walkowicz, L. M., & Reiners, A. 2013, ApJ, 769, 1
Borucki, W., Koch, D. G., & Basri, G. 2011, ApJ, 736, 19
Bottke, W. F., Vokrouhlický, D., Rubincam, D., et al. 2006, AREPS, 34, 157
Caldwell, D. A., Kolodziejczak, J. J., Van Cleve, J. E., et al. 2010, ApJ, 713, L92
Cornish, N. J. 1998, online: http://map.gsfc.nasa.gov/ContentMedia/lagrange.pdf
Dvorak, R., Pilar-Lohinger, E., Schwarz, R., et al. 2004, A&A, 426, L37
Érdi, B., Nagy, I., Sándor, Z., et al. 2007, MNRAS, 381, 1
Fernández, Y. R., Sheppard, S. S., & Jewitt, D. C. 2003, AJ, 126, 3
Fressin, F., Torres, G., Charbonneau, D., et al. 2013, ApJ, 766, 2
Fröhlich, C., Andersen, B. N., & Appourchaux, T. 1997, SoPh, 170, 1
Hippke, M. 2015, ApJ, 806, 51
Hippke, M., & Angerhausen, D. 2015, ApJ, 810, 29
Janson, M. 2013, ApJ, 774, 2
Jenkins, J. M., Caldwell, D. A., & Borucki, W. J. 2002, ApJ, 564, 495
Jewitt, D. C., Trujillo, C. A., & Luu, J. X. 2000, A&A, 120, 2
Johnson, J. A., Aller, K. M., & Howard, A. W. 2010, PASP, 122, 894
Lagrange, J.-L. 1772, Essai sur le problème des trois corps, in: Oeuvres de Lagrange (Paris: Gauthier-Villars)
Laughlin, G., & Chambers, J. E. 2002, AJ, 124, 1
Lissauer, J. J., Marcy, G. W., & Rowe, J. F. 2012, ApJ, 750, 2
Marcos-Arenal, P., Zima, W., De Ridder, J., et al. 2014, A&A, 566, A92
Marzari, F., Scholl, H., Murray, C., et al. 2002, in Origin and Evolution of Trojan Asteroids, ed. W. F. Bottke (Tucson: Univ. Arizona Press)
Moldovan, R., Matthews, J. M., Gladman, B., et al. 2010, ApJ, 716, 1
Murray, N., & Holman, M. 1999, Sci, 283, 5409
Rauer, H., Catala, C., Aerts, C., et al. 2014, ExA, 38, 1
Rowe, J. F., Bryson, S. T., Marcy, G. W., et al. 2014, ApJ, 784, 1
Ruppert, D. R., Wand, M. P., & Carroll, R. J. 2003, Semiparametric Regression (Cambridge: Cambridge Univ. Press)
Sheets, H. A., & Deming, D. 2014, ApJ, 794, 2
Takezawa, K. 2006, Allgemeines Statistisches Archiv, 90, 4
Wolf, M. 1996, AN, 170, 353
Wright, J. T., Fakhouri, O., Marcy, G. W., et al. 2011, PASP, 123, 902
Yoshida, F., & Nakamura, T. 2005, AJ, 130, 6
Zima, W., Arentoft, T., De Ridder, J., et al. 2010, AN, 88, 789